基于 ANN 的 TA15 钛合金 TIG 焊接头拉伸性能模型建立

王　敏，　杨　磊，　魏艳红，　吴　林
（哈尔滨工业大学 现代焊接生产技术国家重点实验室，哈尔滨　150001）

王　敏

摘　要：近 α 型钛合金 TA15 具有较好的综合力学性能，在飞机结构中有广阔的应用前景。针对 TA15 钛合金进行了系统的 TIG 焊试验，并进行了焊接接头拉伸性能测试。在此基础上，基于人工神经网络（ANN）原理对影响 TA15 钛合金 TIG 焊接头拉伸性能的主要参数进行了选取，确定 ANN 的输入和输出参数，建立了 TA15 钛合金 TIG 焊接头拉伸性能 ANN 模型并对模型进行了优化及误差分析。结果表明，最终建立的拉伸性能模型能很好地适用于 TA15 钛合金 TIG 焊接头拉伸性能的模拟，优于传统回归方法。

关键词：人工神经网络；力学性能预测；焊接接头
中图分类号：TG407　　文献标识码：A　　文章编号：0253－360X(2007)12－056－05

0　序　　言

新型近 α 型中强度钛合金 TA15 具有较好的综合力学性能，较好的锻造工艺性能，且热处理工艺简单易行，焊接性能优良。在飞机结构中有广阔的应用前景，具有很高的研究价值[1]。同时由于钛及钛合金结构多用于构件的关键部位，其焊接接头的力学性能往往正是决定关键部位质量的关键因素。因此对焊接接头力学性能的预测及安全性检查是十分必要的。但传统的抽样进行的是破坏性检测，而且更是耗费大量的人力、物力，降低了企业的生产效率及工人的生产积极性。

长久以来，人们试图使用多元回归[2]、模糊数学等技术来预测接头性能。但焊接过程是一个复杂的过程，很多参数难以量化，存在许多不确定性的模糊知识，给预测过程带来了一定的困难。人工神经网络（ANN）是一个高度复杂的非线性动力系统，其除具有一般非线性系统的共性外，还具有其自身的高维性、互连性及自适应或自组织性。因此在预测和模拟焊接接头力学性能方面得到了广泛的研究与应用[3－6]。

但是，目前基于 ANN 的拉伸性能预测模型多存在着一些不足，数据来源于已有的文献资料；缺少具体的有针对性的数据采集试验；模型影响因素考虑不周全；实用价值偏低等。

收稿日期：2007－02－26

为此，作者针对实际生产中 TA15 钛合金焊接条件，进行了系统的试验，比较全面地考虑焊接过程中的影响因素，建立 TA15 钛合金 TIG 焊接头拉伸性能预测模型，将具有比较大的实际应用价值。

1　试验数据采集

试验材料选用 TA15 合金，经 X 射线分析测得所用材料的具体成分如表 1 所示。

表 1　TA15 板材的具体成分（质量分数，%）

Table 1　Chemical composition of TA15 plate

TA15 主要成分				
Ti	Al	Mo	V	Zr
余量	6.84	1.34	1.53	2.18
杂质成分				
Fe	Si	C	H	O	N
0.043	0.080	0.036	0.005	0.061	0.015

试验所用试板为 1.5 mm×80 mm×160 mm 的 TA15 钛板共 80 块。并对试板进行打磨毛刺、酸洗、去除焊接位置的氧化膜等焊前处理。根据前期试验，在制定焊接工艺参数时控制焊接热输入保持在 2.40～9.07 kJ/cm。

试验分 30 组，分别采用不同的焊接工艺参数焊接。焊接设备为美国 Jetline 自动焊接设备并配备

Miller XMT456/9500 焊接电源，电极直径为 2.0 mm。采用喷嘴、正面拖罩、背面三路充氩气对熔池、焊缝及近缝高温区进行全方位保护。

试板按图 1a 所示进行对焊。将焊接完成的试板按预先制定的焊接工艺参数对试板进行焊后热处理，消除焊接应力。再将热处理完毕的试板按图 1b 所示的试样尺寸进行加工。进行拉伸试验的设备为 SHIMADZU AG —100KNG 自动拉伸机。其上下夹头的加载速率均为 10.0 mm/min。

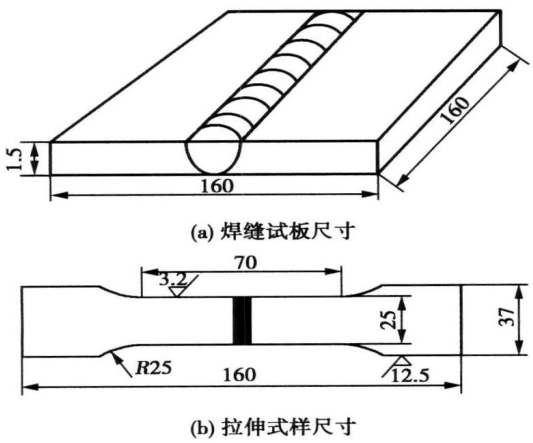

图 1　焊接试板及拉伸试样尺寸(mm)

Fig. 1　Schematic drauling of welded plate and tensile sample

由于拉伸试件的断裂点对最终模型精确度有很大的影响。例如，从试验数据中发现断口在母材处的拉伸试样所测得的断后伸长率值往往要高于断口在焊缝处的情况。因此可以将断裂位置大致分为断在焊缝及母材两种，且分别用数字 1，2 表示，作为模型的一个影响因子。

2　模型建立

预测模型建立分为数据预处理、单个模型训练、组合模型训练及模型优化等几个步骤。

2.1　数据预处理

在建立人工神经网络模型之前，要确定好预测模型的输入及输出参数。通过分析影响接头拉伸性能的因素，将焊接电流、电弧电压、焊接速度、焊后热处理温度、保护气流量及断口位置作为模型的输入参数。将抗拉强度、屈服强度及断后伸长率值作为模型的输出参数。选用三层 BP(反向传播)网络模型及双曲正切函数来建立拉伸性能预测模型。现仅以抗拉强度预测模型为例说明模型的建立过程。抗拉强度模型的网络拓扑结构如图 2 所示。

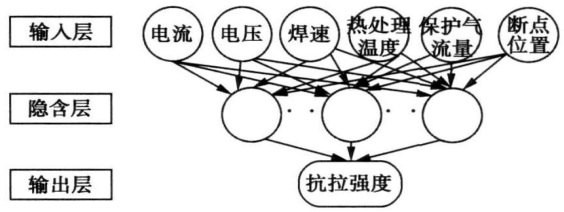

图 2　抗拉强度预测模型的网络拓扑结构

Fig. 2　Topological structure of tensile strength prediction model

联系输入单元和第 i 个隐含单元的转换函数为

$$h_i = \tanh\left(\sum_j w_{ij}x_j + \theta_j\right)。\tag{1}$$

隐含单元和输出单元之间的关系为线性关系，即

$$y = \sum_i w_i h_i + \theta\,,\tag{2}$$

式中：x_j 为第 j 个输入参数；h_i 为第 i 个隐含单元；y 为输出值；w_{ij} 为输入参数 x_j 与隐含单元 h_i 之间的权值；w_i 为隐含单元 h_i 与输出值 y 之间的权值；θ_j 为输入层与隐含层之间的偏差；θ 为隐含层与输出层之间的偏差[7]。因为双曲正切函数是非线性函数，所以该模型能预测非线性联系。

利用试验获得的数据对模型进行训练，即可得到上述权值。输入及输出量之间的非线性关系可以通过调整权值来改变。

抗拉强度预测模型样本数据输入输出参数的最大值、最小值、平均值和均方差如表 2 所示。进行模型训练时将所采集的 84 组数据随机分为训练组数据及测试组数据。测试组数据用来评估模型的优劣性。

2.2　单个模型的训练与测试

经典 BP 算法神经网络采用式(3)作为误差函数，随着学习次数的增加，$|t_j - y_j|$ 越来越小，使函数逼近速度减慢[8]。

$$E_P = \frac{1}{2}\sum_j (t_j - y_j)^2\,,\tag{3}$$

式中：y_j 是预测输出值；t_j 是对应于 y_j 的实测值。该误差函数与隐含单元的数量、测试误差及权重的平方和有关。

人工神经网络经常通过最小测试误差的大小来判断模型的优劣性。但有时利用对数预测误差(LPE)评估神经网络模型更为合适。LPE 值的定义为

$$LPE = \sum_j \left[\frac{\frac{1}{2}(t_j - y_j)^2}{\sigma_j^2} + \log\left(\sqrt{2\pi}\,\sigma_j\right)\right],\tag{4}$$

式中：σ_j 是第 j 组输入参数的不可靠值，LPE 的值越大越好[5]。

表 2 抗拉强度预测模型样本数据分布区间

Table 2 Distribution of tensile strength prediction model' s sample data

	焊接电流 I/A	电弧电压 U/V	热处理温度 T/℃	焊接速度 v/(mm·min^{-1})	保护气流量 q/(L·min^{-1}) 焊枪	托罩	背面	断裂位置	抗拉强度 R_m/MPa
最小值	80.0	8.0	640.0	150.0	10.0	12.0	5.0	1	931.12
最大值	130.0	13.0	750.0	300.0	15.0	18.0	6.0	2	1 073.52
平均值	101.96	10.69	698.93	177.38	12.61	15.00	5.39	1.29	1 010.22
均方差	14.99	1.59	55.19	36.74	2.09	2.55	0.49	0.46	31.94

模型在样本数据确定之后，随机选择 5 个不同的权值作为初始权值，同时训练和测试具有不同隐含层单元数(从 1～20)的多个网络模型。测试误差及对数误差的 LPE 值用来说明每个模型的特征。训练结束后，抗拉强度模型的上述特征如图 3 所示。

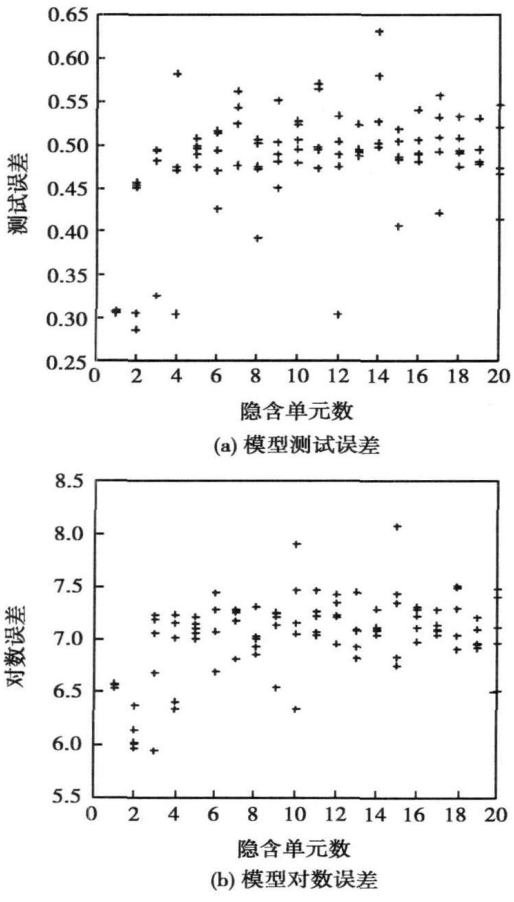

图 3 模型特征与隐含单元数的关系

Fig. 3 Relations between model features and hidden units

由图 3 可以看出，隐含单元较少的模型，相应的噪声值较大；隐含单元数为 2 的模型，测试误差值最小；隐含单元数为 15 的模型，其对数误差 LPE 值最大。而对于 LPE 值，其越大模型的预测能力越好。

2.3 组合模型的训练与测试

用若干模型组合后进行预测，往往能够获得比单个模型更好的预测效果。因此，在单个模型的训练与测试完成之后，还要训练和测试具有不同子模型数的组合模型，并根据组合模型的测试误差来衡量组合模型的性能优劣。这里，组合模型的测试误差类似于组成该模型的所有子模型的测试误差的平均值。训练完毕后，模型的组合误差如图 4 所示。

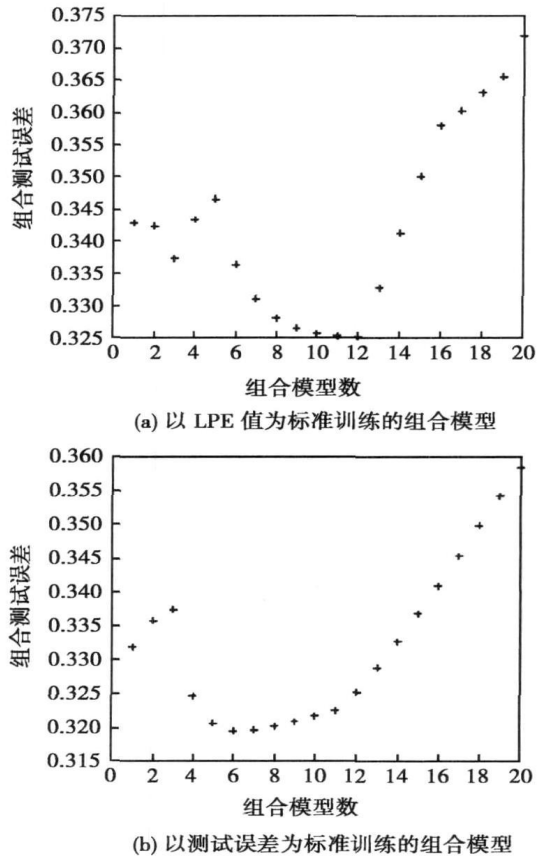

图 4 两个不同形式的组合模型测试误差

Fig. 4 Combined test error with two different types

比较图 4 可知在该模型的组合模型中，由测试误差最小的子模型组成的组合模型比由 LPE 值最大的模型组成的组合模型测试误差小。同时由图 4b 可知，单个模型的最小测试误差为 0.336，而当组合模型的子模型数为 6 时组合模型的测试误差值最小，为 0.319。因此，可以选用以测试误差最小的前 6 个(M1～M6)模型来进行组合模型的训练，建

立模型。

2.4　模型的优化

模型建立后，比较各输入参数对输出参数的影响因子。发现一些影响因子特别小的输入参数，去除这些不必要参数，重新训练，可得到性能更好的模型，即进行降维处理。

抗拉强度模型的各输入参数对输出参数的影响因子直方图如图 5 所示，6 种不同直方图分别代表在上节中进行组合模型训练的 6 个模型。根据图 5，将焊接保护气流量和断点位置剔除，重新训练模型。

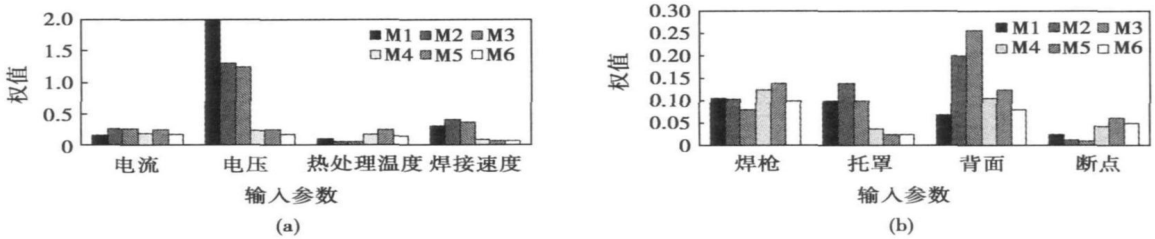

图 5　各输入参数对输出参数的影响权值

Fig. 5　Significant of inputs to outputs

使用所建立的模型进行预测，可以看出各输入参数对输出参数的影响规律及其预测误差带的大小。有时，会发现有些输入参数的预测误差带特别大，甚至于完全掩盖了输入参数对输出参数的影响规律。为了避免这种现象，可以缩小样本数据的覆盖区间，提高样本数据均匀性，从而提高模型的性能。

重新训练后观察预测误差带发现，模型的预测规律性不仅得到了保证，而且缩小了误差带的范围提高了预测精度。优化前后模型误差带变化如图 6 所示。

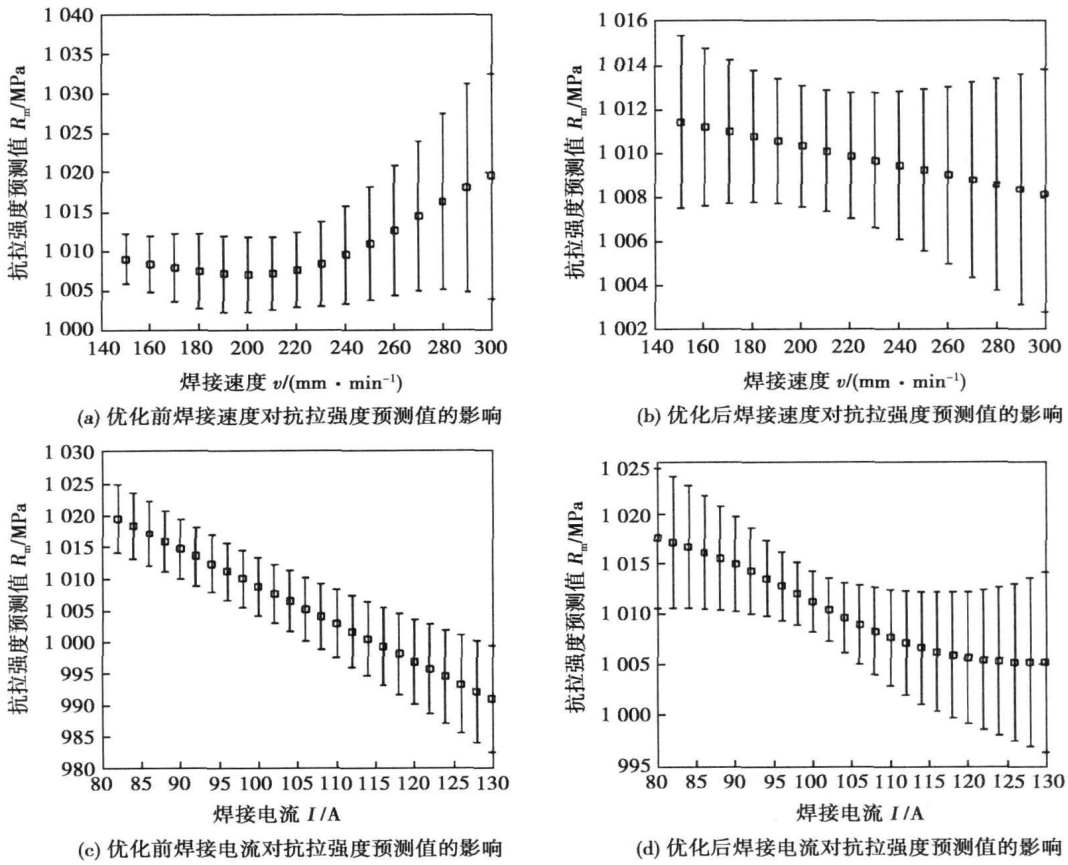

图 6　优化前后抗拉强度预测误差带的变化

Fig. 6　Error band changes of tensile strength prediction between pre and post optimization

3 结 论

(1) 通过 TA15 焊接接头力学性能试验,获得了比较全面的焊接条件与拉伸性能关系数据记录。

(2) 建立了基于人工神经网络的 TA15 钛合金 TIG 焊接头的拉伸性能预测模型。经降维及缩小样本空间的优化处理及重训练后,能很好地拟合现有的试验数据,同时具有很高的预测精度,能很好地满足实际应用的需求。

参考文献:

[1] 李兴无, 沙爱学, 张旺峰. TA15 合金在飞机结构中的应用前景[J]. 钛工业进展, 2003, 20(4—5): 90—94.

[2] 柳百成, 荆 涛, 黄天佑, 等. 铸造工程的模拟仿真与质量控制[M]. 北京: 机械工业出版社, 2001.

[3] Wei Yanhong, Badeshia H K D H, Sourmai T. Mechanical property prediction of commercially pure titanium welds with artificial neural network[J]. Journal of Material Science & Technology, 2005, 21(3): 403—407.

[4] Wei Yanhong, Badeshia H K D H, Sourmai T. Modeling mechanical properties of GTAW welds of commercial titanium alloys with artificial neural network[J]. Transactions of Nonferrous Metals Society of China, 2005, 15(S2): 70—74.

[5] Lalam S H, Bhadeshia H K D H, Mackay D J C. Estimation of mechanical properties of ferritic steel welds, Part 1: yield and tensile strength[J]. Science and Technology of Welding and Joining, 2000, 5(1): 135—147.

[6] 王 敏. 合金钢计算机辅助焊接工艺评定[D]. 哈尔滨: 哈尔滨工业大学, 2003.

[7] Tracey Cool, Bhadeshia H K D H, MacKay D J C. The yield and ultimate tensile strength of steel welds[J]. Materials Science and Engineering, 1997, A223: 186—200.

[8] 石 玗, 樊 丁, 陈剑虹. 神经网络方法的焊接接头力学性能预测[J]. 焊接学报, 2004, 25(2): 73—76.

作者简介: 王 敏, 女, 1963 年出生, 博士研究生, 教授, 沈阳飞机工业(集团)有限公司副总冶金师, 研究员级高级工程师, 公司首席专家。主要研究方向为计算机技术在焊接中的应用。获国家及省部级科技奖 5 项, 发表论文 4 篇。

Email: sywm@163.com

Abstract: The paper studied principle of arc produced heat in VPPA and analysed how welding parameters influence arc heat from physical properties of arc on Al alloy. It is shown that dissymmetrical electrode properties have great influence on produced heat of arc in positive and negative times. When Al alloy is used to be negative electrode, negative voltage produced more heat. Different parameters of welding current and lasting times are very important factors to produce heat in positive and negative times.

Key words: variable polarity plasma welding; electrical properties; aluminum alloy

Detection method of spot welding based on fractal and support vector machine LIU Pengfei, SHAN Ping, LUO Zhen (School of Materials Science and Engineering, Tianjin University, Tianjin 300072, China). p38—42

Abstract: Because of characteristic of fractal dimension which present quantitatively describing of complexity of a sample data series and remarkable advantage of support vector machine (SVM) in small sample classification and regression, fractal dimension of signal data series is adopted as eigenvectors, and a novel detection method based on fractal and SVM is presented. Two models based on SVM are constructed. One is about flatters of spot welding and the other is about defect of nugget size. A array of SVM is consist of these two models. The array is used to detect the two defects synchronously. It is shows that this new method fits for nondestructive detection of spot welding from analysis of experiment results. This array of SVM can detect the two defects of flatters and the little nugget size better in process of spot welding.

Key words: fractal; support vectors machine; detection; spot welding; flatter

Vibration frequency characters of chip and bonding on thermosonic flip chip bonding WANG Fuliang, HAN Lei, ZHONG Jue (School of Mechanical and Electronical Engineering, Central South University, Changsha 410083, China). p43—46

Abstract: The vibration velocity of tool tip and chip on thermosonic flip chip (TSFC) bonding was monitored with a laser Doppler vibrometer, and the "stall" phenomena was observed from the virtual value curve of vibration velocity, i. e., after the TSFC bonding started a fever milliseconds, the chip velocity decreases suddenly, while the tool tip velocity still increases. Stall indicated that the bump/pad interface has formed initial bonding strength. And the frequency characters of the vibration velocity signals were also obtained. It is found that the 3rd harmonics of chip vibration velocity signal indicates the stall phenomena, i. e., when the 3rd harmonics appeared, the stall happens. Experiment results show that little bonding force is good for produce stall.

Key words: thermosonic flip chip bonding; laser Doppler vibration measurement; spectral analysis

Effects of immediate water cooling and normalization after welding on microstructure and hardness of heat affected zone of ultra-fine grain steels welded joint ZHANG Guifeng[1], MIAO Huixia[1], ZHANG Jianxun[1], PEI Yi[1], WANG Jian[2], ZHANG Yantao[3] (1. School of Material Science and Engineering, Xi' an Jiaotong University, Xi' an 710049, China; 2. Technical Center of Anshan Iron and Steel Group Corporation, Anshan 114000, Liaoning, China; 3. Shandong Electric Power Construction No. 1 Project Company, Jinan 250100, China). p47—50

Abstract: To refine the grain size of the coarse grain heat affected zone (CGHAZ) in the gas tungsten arc welded joints of ultra-fine grain (UFG) steels of 400 MPa strength, the immediate water cooling before transformation completion and normalization after welding were performed. Their effects on the microstructure and hardness of the HAZ were investigated. The results show that although the grain size of CGHAZ does not decrease for the immediate water cooling, the width of CGHAZ decreases compared with the air cooling condition. The effective grain sizes in CGHAZ are significantly refined by first time normalization treatment after welding, while the grain sizes in the fine grain heat affected zone (FGHAZ) become coarser than those before normalization. The hardness of HAZ of the joint subjected to immediate water cooling is higher than that of the joint subjected to air cooling. The whole hardness of each joint after normalization decreases much. There is a favorable hardness match between the HAZ and the original base metal after first normalization treatment only for the immediate water cooling joint. Therefore, the immediate water cooling followed by one time normalization is recommended to refine the grain size in CGHAZ and to make the hardness of HAZ close to that of original parent materials.

Key words: ultra-fine grain steels; heat affected zone; coarse grain heat affected zone; normalization; hardness

Distribution and diffusion mechanism of Sn in interface of ZA alloy soldered joints LIU Xiuzhong, LI Shitong, CHEN Libo (School of Material Science and Engineering, Shandong University, Jinan 250061, China). p51—55

Abstract: Microstructure and its characteristic of ZA soldered joints, distribution of Sn elemont and reaction product of Sn in interface of ZA alloy soldered joints are studied by optical microscope, scanning electron microscope and electron probe microanalysis, reskectively. The results show that Sn mainly diffuses by volume diffusion and forms a wide diffusion zone. Sn in interface also reacts with some elements in parent metal. New phases such as α—CuSn and $Cu_{20}Sn_6$ are formed. The diffusion and reaction of Sn will be propitious to the bonding strengths and mechanical properties of soldered joints, which can satisfy the service performance of soldered joints.

Key words: ZA alloy; soldering; interface; diffusion of Sn

ANN prediction models for tensile properties of TIG welded

joints of TA15 titanium alloys WANG Min, YANG Lei, WEI Yanhong, WU Lin (State Key Laboratory of Advanced Welding Production Technology, Harbin Institute of Technology, Harbin 150001, China). p56—60

Abstract: Near-alpha TA15 titanium alloy has good mechanical properties which has a wide application in airframe. Systemic TIG (tungsten inert-gas) welding experiments were performed for TA15 titanium alloy and the tensile tests of their welded joints were also carried out. Main factors were then selected after relating the parameters to tensile properties based on the principle of artificial neural network (ANN). Finally, the input and output parameters were confirmed and the ANN prediction models for tensile properties of titanium alloys TA15 TIG welded joints were established. Those models were then optimized and the model errors were analyzed. It showed that the prediction models, better than the traditional regression method, could be well used to predict tensile properties of titanium alloys TA15 TIG welded joints.

Key words: artificial neural networks; mechanical properey prediction; welded joint

Growth behavior of compounds at Sn3.5Ag0.5Cu/Ni under thermal-shearing cycling QI Lihua, HUANG Jihua, ZHAO Xingke, ZHANG Hua (School of Material Science and Engineering, Beijing University of Science and Technology, Beijing 100083, China). p61—64

Abstract: The atoms diffusion and growth behavior of intermetallic compound (IMC) at Sn3.5Ag0.5Cu/Ni interface after thermal-shearing cycling (25— 125 ℃) were investigated, which was compared to compound growth behavior under isothermal aging condition. The results showed that there is a type of $(Cu_xNi_{1-x})_6Sn_5$ IMC formed at the interface after reflowing, and the morphology of compound changes from scallop-like with the cycling increasing. There is another kind of compound $(Ni_xCu_{1-x})Sn_3$ formed surrounding $(Cu_xNi_{1-x})_6Sn_5$ after 200 cycles and grow up rapidly as planar-like. As the thermal-shearing cycling increasing, Ag_3Sn formed uniform particles after reflowing congregates to grow up to chunk-like in the solder. The IMC at the interface growth follows a parabolic growth kinetiscs with the thermal-shearing cycling increasing, implying that it was controlled by Cu atom diffusion.

Key words: thermal-shearing cycling; intermetallic compounds; solder; interface

Threshold calibrating of 6D touching force in welding seam identifying LIU Lijun[1,2], DAI Hongbin[2], GAO Hongming[3], WU Lin[3] (1. Ningbo Institute of Technology, Zhejiang University, Ningbo 315100, Zhejiang, China; 2. School of Material Science & Engineering, Harbin University of Science and Technology, Harbin 150080, China; 3. State Key Laboratory of Advanced Welding Production Technology, Harbin Institute of Technology, Harbin 150001, China). p65—68

Abstract: The welding seam identifying (WSI) is one prerequisite for remote welding. The welding seam is usually identified by vision sensor. While the study on WSI based on 6 dimensional (6D) force is less reported. When the 6D force sensor fixed on welding robot moves along with space welding seam, the weight of probe fixed on 6D force sensor will influence on 6D force value of WSI. As 6D force probe does not contact with welding seam, the blind section of 6D force is calibrated in different space position by testing 6D force value in $x-z$, $y-z$ plane. When 6D force probe contacts with welding seam, the threshold of 6D touching force is calibrated in different space position. The experiment of WSI efficiency is achieved by use of this technologies. The experimental results show that the efficiency of WSI is improved sixty percent comparing with manual WSI. It provides condition for the welding seam identified quickly and exactly.

Key words: welding seam identifying; 6 dimensional touching force; threshold calibrating

Optimization of mechanical properties prediction models of welded joints combined neural network with genetic algorithm DONG Zhibo[1], WEI Yanhong[2], Zhan Xiaohong[1], WEI Yongqiang[1] (1. State Key Laboratory of Advanced Welding Technology Production, Harbin Institute of Technology, Harbin 150001, China; 2. Department of Material Science and technology, Nanjing University of Aeronautics and Astronautics, Nanjing 210016, China). p69—72

Abstract: Genetic algorithm was used to optimize the back-propagation neural network connection weights and improve the models predicted precision and generalization ability on the basic of the mechanical properties prediction models of welded joints established with back-propagation neural network. The performance analysis shows that the predicted trend agrees well with the previous research work and the predicted error is less than 5%. It is obvious that the models will be more applicable and valuable in the practice with the enlargement of database and the data-covering space.

Key words: genetic algorithm; neural network; back propagation; mechanical properties prediction model

Two typical anti-interference designs of digital tungsten inert-gas welding inverter WANG Shouyan, YAO Heqing, FAN Xinghui, YIN Yongzhen (College of Mechanical and Electrical Engineering, Hohai University, Changzhou 213022, Jiangsu, China). p73—76, 80

Abstract: The causes of interference in the propagation of the bat-handle switch and arc voltage signal are pointed and their affections to arc welding machine are analyzed. Two useful anti-interference transmission circuits toward the two signals are designed. Drooping characteristic pulse transformer is used to ensure isolation between working signal and interfering signal in bat-handle switch signal transmission circuit. LC filter and linear-optocoupler are used